*Article*

# Studying the Recurrent Sequence Generated by Power Function using QUATTRO-20

Jelena Kozmina*, Alytis Gruodis
Department of IT, Vilnius Business College, Kalvarijų g. 129-401, LT-08221 Vilnius, Lithuania
* Corresponding author, e-mail: *jelena.kozmina@gmail.com*

Received: 4 November 2023
Accepted: 10 December 2023
Online: 30 December 2023

**Abstract.** We presented the bifurcational diagram of power function $\Phi(x) = r \cdot x \cdot (1 - x^2)$ which could be treated as first approximation of trigonometric function $F(x) = r \cdot x \cdot \cos x$. Using second composite $\Phi^2(x)$ in analytical form and solving 8-th degree polynomial equation bifurcational diagram with period doubling 1, 2, 4 was obtained and attractors were established. Analytical solutions of expressions $x = \Phi^2(x)$ allows us to establish the fixed point attractors and periodic attractors in interval (-$\sqrt{5}$, $\sqrt{5}$). Bifurcation diagram obtained analytically was compared with its aproximate analogue Finite State diagram.

**JEL:** C25.

**Keywords:** recurrent sequence; power function; fixed point attractor; periodic attractor; Finite State Diagram; Bifurcation diagram; index of Lyapunov exponent; CobWeb plot.

**Citation:** Jelena Kozmina, Alytis Gruodis (2023) Studying the Recurrent Sequence Generated by Power Function using QUATTRO-20. – *Applied Business: Issues & Solutions* 2(2023)28–36 – ISSN 2783-6967.
https://doi.org/10.57005/ab.2023.2.4

## Introduction

Recurrent sequences can be important in various fields of physics, chemistry, engineering, and informatics in the context of modeling of periodic or oscillatory behavior which orccur at visualization of reaction or engine cycle, cipher/key generation, big data maintening etc.

Trigonometric functions (sine and cosine) naturally represent an oscillatory behavior (vibrations, waves, etc) with periodic components. Phenomenon of recurrence allows describing the evolution of complex systems in several dynamical regimes where the characteristic regime parameters repeat or oscillate over time [1, 2]. This is particularly relevant in audio processing, where signals often exhibit the repeating patterns.

Recurrent sequences with trigonometric functions can arise in solutions to certain differential equations. These equations may model physical phenomena where both recurrence and periodicity play a significant role [3, 4].

Typical tasks of BigData requires the analysis of data collections, where data sampling was provided over time. Usage of recurrent functions with trigonometric terms can help capture patterns and trends that repeat at regular/pseudoregular intervals [5, 6].

Usage of recurrent sequencies with trigonometric terms in Artificial Neural Network and Machine Learning could be estimated as the novel implementation of processing of the data sequences [6-9]. Trigonometric functions can be incorporated into the activation functions or hidden states of Artificial Neural Networks to represent the time-domain or temporal dependencies with periodic characteristics.

Analysis technique is known [10-12]: Finite State Diagram, Bifurcation diagram, distribution of index of Lyapunov exponent, CobWeb plot for different composites of function $F(x)$: $F^2(x)$, $F^3(x)$, $F^4(x)$. This solution pathway was shown for classical Verhulst equation $F(x) = r \cdot x \cdot (1 - x)$ presented in Refs. [10, 11] as standard manipulation in analytical form using polinomial behaviour. Unfortunately, for recurrent trigonometric functions, possibility to express the composites of high order $F^2$, $F^3$, $F^4$ could be realized in approximate form only.

This work is devoted to understanding the specific context in which recurrent sequences generated by the trigonometric functions $F(x) = r\cdot x\cdot \cos x$ could be replaced with corresponding polynomial function $\Phi(x) = r \cdot x \cdot (1 - x^2)$ Depending on the field and application, these functions can provide accurate and efficient dynamical representations of real-world phenomena with periodic behavior.

## 1. Literature review

**Recurrent relations.** Recurrent relation expresses the relationship between the terms of a sequence, when the previous term predeterms the behaviour of the current. Usage of the mentioned recursive technique is popular due to simplicity to control the generation. Dosly et al [13] presented so called trigonometric transformation technique for recurrence relations. Brooke et al [14] described several forms of second-order linear Recurrent relation, which satifies the requested features: jump from a sequence with period $k$ to second-order linear Recurrent relation. In that case, three distinct non-trivial periods will be generated. Farris et al [15] proved, that for certain families of functions $f$ and $g$, a sequence generated by a recurrent relation

$$a_{n+1} = f(n) \cdot a_n + g(n) \cdot a_{n-1} \qquad (10)$$

is Benford for all initial values. Importance of Benford law [16] is well known. It describes a natural phenomenon from many real-world datasets. It reflects a pattern that emerges in naturally occurring numerical data, such as physical constants, parameters of biological systems, etc. By analysing this distribution, it is possible to distinguish between sequences related to the naturally occuring system and formula-generated data.

**Indicators of chaos.** Generally, pure chaotic manner of recurrent relation could be established from natural processes only [16]. As mathematical models, the Lorenz system, the Henon map as well as logistic map are well known [17]. Each of these models has its own set of equations. Andrianov et al [17] use various variants of Verhulst-like ordinary differential equations and ordinary difference equations. Several examples of deterministic discretization and chaotic continualization (procedure is based on Padé approximants) are analysed. Characteristic parameters of chaotic dynamical systems as the Lyapunov exponents and the Lyapunov dimensions were presented and discussed.

Gutierrez et al [18] analyzed Verhulst logistic equation and a couple of forms of the corresponding logistic maps. In particular, they presented the map

$$x_{n+1} - x_n = r \cdot x_n \cdot (1 - x_{n+1}) \qquad (11)$$

or in usual form:

$$x_{n+1} = \frac{(1+r)x_n}{1+r\cdot x_n} = 1 - \frac{1-x_n}{1+r\cdot x_n} \tag{12}$$

which is identical to the logistic equation from the standpoint of the general Riccati solution.

Ragulskis et al [19] presented the concept of the Hankel rank of a solution of the discrete nonlinear dynamical system. Computation of ranks of subsequences of solutions helps to identify and assess the sensitivity of the system to initial conditions: stability or convergence properties.

Hikihara et al [20] presented explicit historical review of the systems of deterministic chaos. They claim that unpredictability is due to sensitive dependence on initial conditions caused by rapid divergence of neighbouring solutions. This property is quite common in nonlinear differential equations with three or more variables, invertible maps in two or more dimensions, and all non-invertible maps. Chaotic dynamics is locally expansive in one or more directions in phase space and contractive in the remaining dimensions. Only in the last 50 years, the significant applications are presented for investigation in the biological and life sciences. Analytical, geometrical, and computational methods have been developed to detect and characterize chaotic sets, and experiments have confirmed that they appear in a variety of real systems.

Ditto et al [21] presented description if investigations in chaotic system, in particular, problems of Artificial Intelligence, such as Artificial Neural Network, fuzzy logic, and genetic algorithms can be employed together with chaotic systems (e.g., neural networks and chaos, or neural networks and fuzzy logic and chaos.) Components of hybrid systems complement each other creating new approaches to solve problems.

Nosrati et al [22] investigated the biological systems in the real world using the singular system theory and fractional calculus. Some fractional-order singular biological systems are established, and some qualitative analyses of proposed models are performed. It was established that presence of fractional order changes the stability of the solutions and enriches the dynamics of system. In comparison to standard model, fractional-order singular biological systems exhibit instability phenomena (in term of bifurcation).

Generally, classic chaos-detection tools are highly sensitive to measurement noise. Toker et al [23] presented novel tool which combine several classical tools into an automated processing pipeline, and show that this pipeline can detect the presence (or absence) of chaos in noisy recordings, even for difficult cases.

Fehrle et al [24] presented polynomial chaos expansion method for series expansion of uncertain model inputs. Suitability of polynomial chaos expansion for computational economics is discussed.

**Cryptography.** Recurrent relations are important in cryptographic applications because the generation of pseudorandom numbers play a crucial role in cryptographic protocols and algorithms. Estimation of sequence quality of pseudorandom numbers [25] must be done due to security restrictions. Alawida et al [26] presented a hybrid chaotic which uses cascade and combination methods as a nonlinear chaotification function. Analysis shows that enhanced maps have a larger chaotic range, low correlation, uniform data distribution and better chaotic properties. Several simple pseudorandom number generators are designed based on a classical map and its enhanced variant.

# 2. Sequence generated by power function

We would like to study the properties of sequence

$$x_{t+1} = F(x_t), \quad t = 0,1,2,\dots\ , \tag{13}$$

where

$$F(x) = r\cdot x\cdot \cos x \tag{14}$$

for different values of parameter $r$. Anticipating the difficulties awaiting us, let us start with the approximation of the function $\cos x$ using MacLaurin series. The explicit form the Maclaurin series of a function $\cos x$ is presented below:

$$\cos x = \sum_{n=0}^{\infty} \frac{(-1)^n}{(2n)!} x^{2n} = 1 - \frac{x^2}{2} + \frac{x^4}{24} - \frac{x^6}{720} + \dots\ . \tag{15}$$

The Maclaurin series is used to create a polynomial function

$$\cos x \approx 1 - \frac{x^2}{2}. \tag{16}$$

Using polynomial function $G(x)$

$$G(x) = r\cdot x\cdot \left(1 - \frac{x^2}{2}\right) \tag{17}$$

we generate the sequence

$$x_{t+1} = r\cdot x_t\cdot \left(1 - \frac{x_t^2}{2}\right), \quad t = 0,1,2,\dots\ . \tag{18}$$

Transforming Eq.(18)

$$\frac{x_{t+1}}{\sqrt{2}} = r\cdot \frac{x_t}{\sqrt{2}}\cdot \left(1 - \left(\frac{x_t}{\sqrt{2}}\right)^2\right) \tag{19}$$

and using the substitution

$$\frac{x_t}{\sqrt{2}} \to x_t \tag{20}$$

leads us to the sequence

$$x_{t+1} = r\cdot x_t\cdot (1 - x_t^2), \tag{21}$$

or

$$x_{t+1} = \Phi(x_t), \tag{22}$$

where

$$\Phi(x) = r\cdot x\cdot (1 - x^2). \tag{23}$$

The function $\Phi(x)$ reaches the maximum value $\frac{2r}{3\sqrt{3}}$ on the segment [–1,1] at the point $x$=$\frac{1}{\sqrt{3}}$ and the minimum value $-\frac{2r}{3\sqrt{3}}$ on the segment [–1,1] at the point $x$=$-\frac{1}{\sqrt{3}}$. So function $\Phi(x)$:[–1,1]→[–1,1] if

$$\left|\frac{2r}{3\sqrt{3}}\right| \le 1. \tag{24}$$

This fact imposes restriction on $r$:

$$r \in \Big[-\frac{3\sqrt{3}}{2}, \frac{3\sqrt{3}}{2}\Big], \qquad \frac{3\sqrt{3}}{2} \approx 2.598 < 2.6. \tag{25}$$

# 3. Fixed point attractors

We know [10,12] that if we want to find fixed point attractor of the sequence $x_{t+1}$=$\Phi(x_t)$ then we have to solve the equation $x$=$\Phi(x)$. The function $\Phi(x)$ has to be a contracting map in a closed interval and absolute value of the derivative of function $\Phi(x)$ calculated at the solution of equation $x = \Phi(x)$ have to be less then 1.
We find the fixed points of function $\Phi(x)$ by solving the equation

$$x = r\cdot x\cdot (1 - x^2). \tag{26}$$

This equation has three solutions:

$$x = 0, \quad x = \pm\sqrt{\frac{r-1}{r}}. \tag{27}$$

Now we calculate the derivative of $\Phi(x)$:

$$\frac{d\Phi(x)}{dx} = r \cdot (1 - 3x^2). \tag{28}$$

At point $x$=0

$$\left| \frac{d\Phi}{dx}\bigg|_{x=0} \right| = |r|. \tag{29}$$

If $|r|$<1 then point $x$=0 must be titled as fixed point attractor. Another two solutions of equation $x$=$\Phi(x)$ are $x$=$\pm\sqrt{\frac{r-1}{r}}$.

$$\left| \frac{d\Phi}{dx}\bigg|_{x=\pm\sqrt{\frac{r-1}{r}}} \right| = \left| r \cdot \left(1 - 3\frac{r-1}{r}\right) \right| = \left| 3 - 2r \right|, \tag{30}$$

$$|3 - 2r| < 1 \quad \Leftrightarrow \quad 1 < r < 2. \tag{31}$$

It means that points

$$x = \pm\sqrt{\frac{r-1}{r}} \tag{32}$$

are the fixed point attractors for 1<$r$<2. Note if $r$=1.5 then

$$x = \pm\sqrt{\frac{r-1}{r}} = \pm\sqrt{\frac{1.5-1}{1.5}} = \pm\sqrt{\frac{1}{3}} \approx \pm 0.57735269 \tag{33}$$

and

$$\left| \frac{d\Phi}{dx}\bigg|_{x=\pm\sqrt{\frac{1}{3}}} \right| = 3 - 2 \cdot 1.5 = 0. \tag{34}$$

Figs. 1, 2, 3 represent graphical solutions of two functions: $y = x$ and $y = \Phi(x)$ at different $r$: $r$=1.5, $r$=1.9, $r$=2.2 respectively. For $r$=1.5 (Fig. 1), three crossing points are present, but only two of them $x$=$\pm\sqrt{\frac{1}{3}}$≈0.58 are fixed point attractors (tangent lines are parallel to $x$ axis). For $r$=1.9 (Fig. 2), three crossing points are present, but only two of them $x$=$\pm\sqrt{\frac{9}{19}}$≈0.69 are fixed point attractors. (tangent lines are not parallel to $x$ axis). For $r$=2.2 (Fig. 3), three crossing points are present, including $x$=$\pm\sqrt{\frac{6}{11}}$≈0.74, but none of them are fixed point attractors. Value $r$=2.2 is out of previously established interval 1<$r$<2.

## 4. Periodic attractors

We know that

$$x_{t+2} = \Phi(x_{t+1}) = \Phi(\Phi(x_t)) = \Phi^2(x_t), \tag{35}$$

where

$$\Phi(x) = r \cdot x \cdot (1 - x^2) = r \cdot (x - x^3). \tag{36}$$

Let us express the second order composite $\Phi^2(x)$:

$$\Phi^2(x) = \Phi(\Phi(x)) = r \cdot \left(r \cdot (x - x^3) - \left(r \cdot (x - x^3)\right)^3\right) = \tag{37}$$

$$= r^2 \cdot x \cdot (1 - x^2) \cdot \left(1 - r^2 \cdot x^2 \cdot (1 - x^2)^2\right). \tag{38}$$

Let us find the fixed points of the function $\Phi^2(x)$. To find them we solve equation $x$=$\Phi^2(x)$:

$$x = r^2 \cdot x \cdot (1 - x^2) \cdot \left(1 - r^2 \cdot x^2 \cdot (1 - x^2)^2\right). \tag{39}$$

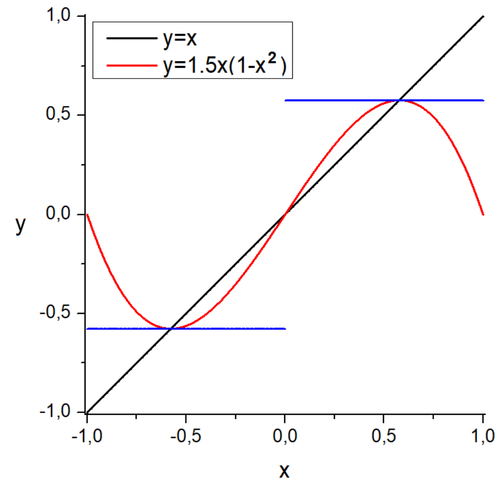


Fig. 1. $y = x$ and $y = \Phi(x)$ at $r$=1.5 (interval 1<$r$<2). Three crossing points, but only two of them (approximate values – 0.58 and 0.58) are fixed point attractors (tangent lines are parallel to $x$ axis).

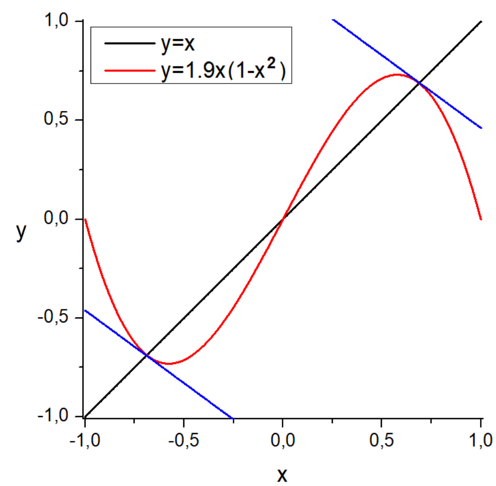


Fig. 2. $y = x$ and $y$=$\Phi(x)$ at $r$=1.9 (interval 1<$r$<2). Three crossing points, but only two of them (approximate values – 0.69 and 0.69) are fixed point attractors.

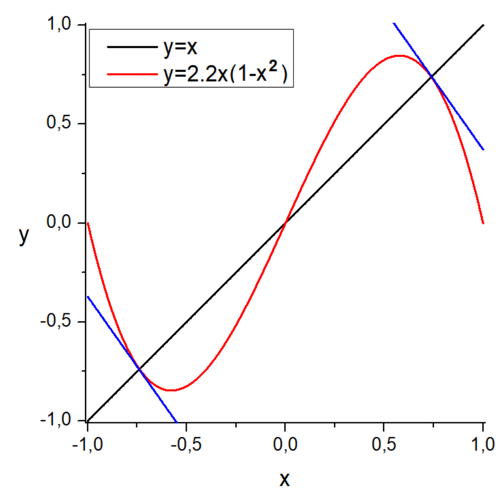


Fig. 3. $y = x$ and $y = \Phi(x)$ at $r$=2.2 (out of interval 1<$r$<2). Three crossing points, but none of them are fixed point attractors.

Table 1. Horner's scheme for $z$=$r$–1.

| | | | | | |
|---|---|---|---|---|---|
| | 1 | $-3r$ | $3r^2$ | $-r^3-r$ | $r^2-1$ |
| $r-1$ | ↓ | + <br> $r-1$ <br> = | + <br> $-2r^2+r+1$ <br> = | + <br> $r^3-1$ <br> = | + <br> $-(r^2-1)$ <br> = |
| | 1 | $-2r-1$ | $r^2+r+1$ | $-r-1$ | 0 |

Table 2. Horner's scheme for $z$=$r$+1.

| | | | | |
|---|---|---|---|---|
| | 1 | $-2r-1$ | $r^2+r+1$ | $-r-1$ |
| $r+1$ | ↓ | + <br> $r+1$ <br> = | + <br> $-r^2-r$ <br> = | + <br> $r+1$ <br> = |
| | 1 | $-r$ | 1 | 0 |

One solution is $x$=0. To get the other solutions we have to solve the equation

$$r^2 \cdot (1-x^2) \cdot \Big(1 - r^2 \cdot x^2 \cdot (1-x^2)^2\Big) = 1. \tag{40}$$

We transform it to the form of $8^{th}$-power equation:

$$r^2 \cdot (1-x^2) \cdot \Big(1 - r^2 \cdot x^2 \cdot (1-2x^2+x^4)\Big) = 1, \tag{41}$$

$$(1-x^2) \cdot \left(r^2 - r^4x^2 + 2r^4x^4 - r^4x^6\right) = 1, \tag{42}$$

$$r^4x^8 - 3r^4x^6 + 3r^4x^4 - r^2(r^2+1)x^2 + r^2 - 1 = 0. \tag{43}$$

We know if $\Phi(x) = x$ then

$$\Phi^2(x) = \Phi(\Phi(x)) = \Phi(x) = x. \tag{44}$$

It means that the solutions of the equations $\Phi(x) = x$ are the solutions of the equations $\Phi^2(x)$=$x$. Let us use substitution $rx^2$=$z$, then we have to solve equation

$$z^4 - 3rz^3 + 3r^2z^2 - r(r^2+1)z + r^2 - 1 = 0. \tag{45}$$

$\Phi(x) = x$ for $x = \pm\sqrt{\frac{r-1}{r}}$, hence $z = rx^2 = r-1$ is the root of the equation

$$z^4 - 3rz^3 + 3r^2z^2 - r(r^2+1)z + r^2 - 1 = 0. \tag{46}$$

We use Horner's scheme presented in Table 1 and get the third power equation

$$z^3 - (2r+1)z^2 + (r^2+r+1)z - r - 1 = 0. \tag{47}$$

Let us check $z = r+1$ using Horner's scheme again - see Table 2. Having applied the Horner scheme we were convinced that $z = r+1$ is a solutions of Eq.(47). Now we have to solve the second power equation

$$z^2 - rz + 1 = 0. \tag{48}$$

The solutions of this equations are

$$z = \frac{r \pm \sqrt{r^2-4}}{2}. \tag{49}$$

We got four solutions of equation

$$z^4 - 3rz^3 + 3r^2z^2 - r(r^2+1)z + r^2 - 1 = 0, \tag{50}$$

$$z = r-1, \quad z = r+1, \quad z = \frac{r \pm \sqrt{r^2-4}}{2}. \tag{51}$$

These four solutions give us eight solutions of Eq.(43). Note that we used substitution $rx^2$=$z$, hence $x^2$=$z/r$, and

$$x_{1,2} = \pm\sqrt{\frac{r-1}{r}}, \quad x_{3,4} = \pm\sqrt{\frac{r+1}{r}}, \quad x_{5,6,7,8} = \pm\sqrt{\frac{r \pm \sqrt{r^2-4}}{2r}}. \tag{52}$$

To check which of these points are attracttors we need to count the value of first derivative of $\Phi^2(x)$ and make sure that at each of these points belongs to the interval (-1,1). For function

$$\Phi^2(x) = r^2 \cdot \Big((x-x^3) - r^2(x-x^3)^3\Big) \tag{53}$$

let's calculate the first derivative with respect to $x$:

$$\frac{d\Phi^2(x)}{dx} = r^2 \cdot (1-3x^2) \cdot \Big(1 - 3r^2x^2 \cdot (1-x^2)^2\Big). \tag{54}$$

For solution $x_{1,2}$

$$x_{1,2}^2 = \frac{r-1}{r}, \qquad 1-3x_{1,2}^2 = \frac{3-2r}{r}, \qquad (1-x_{1,2}^2)^2 = \frac{1}{r^2}, \qquad 1-3r^2x^2\cdot(1-x^2)^2 = \frac{3-2r}{r}, \tag{55}$$

then

$$\frac{d\Phi^2(x)}{dx}\Big|_{x=\pm\sqrt{\frac{r-1}{r}}} = (3-2r)^2. \tag{56}$$

The first derivative of $\Phi^2(x)$ calculated at points $x_{1,2}$ have to be less than 1:

$$\frac{d\Phi^2(x)}{dx}\Big|_{x=\pm\sqrt{\frac{r-1}{r}}} = (3-2r)^2 < 1. \tag{57}$$

This takes place if $r$∈(1,2). Thus we have established that points

$$x_{1,2} = \pm\sqrt{\frac{r-1}{r}} \tag{58}$$

are fixed point attractors if $r$∈(1,2).
Solutions

$$x_{3,4} = \pm\sqrt{\frac{r+1}{r}} \tag{59}$$

is defined if $r$<–1. Similarly we can calculate that

$$\frac{d\Phi^2(x)}{dx}\Big|_{x=\pm\sqrt{\frac{r+1}{r}}} = (3+2r)^2 < 1 \tag{60}$$

if $r$∈(–2,–1). Hence, points $x_{3,4}$ are fixed point attractors if $r$∈(–2,–1).
To simplify the assessment of the derivative of the function $\Phi^2(x)$ at the points

$$x_{5,6,7,8} = \pm\sqrt{\frac{r\pm\sqrt{r^2-4}}{2r}} \tag{61}$$

we will use Eq.(40)

$$r^2\cdot(1-x^2)\cdot(1-r^2\cdot x^2\cdot(1-x^2)^2) = 1 \tag{62}$$

from which these solutions were obtained. We can transform this equation

$$-r^2\cdot x^2\cdot(1-x^2)^2 = \frac{1}{r^2\cdot(1-x^2)} - 1 \tag{63}$$

and substitute it into expression of first derivative of $\Phi^2(x)$ with respect to $x$. For $x = x_{5,6,7,8}$ we get

$$\frac{d\Phi^2(x)}{dx}\Big|_{x=\pm\sqrt{\frac{r\pm\sqrt{r^2-4}}{2r}}} = r^2\cdot(1-3x^2)\cdot(1-3r^2x^2\cdot(1-x^2)^2) = \tag{64}$$

$$= r^2\cdot(1-3x^2)\cdot\Big(\frac{3}{r^2\cdot(1-x^2)} - 2\Big) = \tag{65}$$

$$= \frac{(1-3x^2)(3-2r^2+2r^2x^2)}{1-x^2}. \tag{66}$$

We have to solve the inequality

$$\left|\frac{d\Phi^2(x)}{dx}\Big|_{x=\pm\sqrt{\frac{r\pm\sqrt{r^2-4}}{2r}}}\right| < 1. \tag{67}$$

If $x$∈(–1,1) then 1–$x^2$>0. For $x = x_{5,6,7,8}$ we get Ineq.(68)

$$-1+x^2 < 3-2r^2-9x^2+8r^2x^2-6r^2x^4 < 1-x^2 \tag{68}$$

which leads us to following system of inequalities:

$$\begin{cases} 1-r^2-4x^2+4r^2x^2-3r^2x^4 & <0, \\ 2-r^2-5x^2+4r^2x^2-3r^2x^4 & >0. \end{cases} \tag{60}$$

For

$$x_{5,6}=\pm\sqrt{\frac{r+\sqrt{r^2-4}}{2r}} \tag{61}$$

we have

$$x^2=\frac{r+\sqrt{r^2-4}}{2r}. \tag{62}$$

Substitute Eq.(62) into first inequality of system - Ineq.(60):

$$1-r^2-2\cdot\frac{r+\sqrt{r^2-4}}{r}+2r(r+\sqrt{r^2-4})-\frac{3}{2}(r^2+r\sqrt{r^2-4}-2)<0, \tag{63}$$

$$2-\frac{1}{2}r^2-2\frac{\sqrt{r^2-4}}{r}+\frac{1}{2}r\sqrt{r^2-4}<0, \tag{64}$$

$$\frac{r(4-r^2)-(4-r^2)\sqrt{r^2-4}}{r}<0, \tag{65}$$

$$\frac{(4-r^2)(r-\sqrt{r^2-4})}{r}<0. \tag{66}$$

If $r$>2 then $r$–$\sqrt{r^2-4}>0$ and 4–$r^2<0$, hence $r\in$(2,+$\infty$).
If $r$<–2 then $r$–$\sqrt{r^2-4}<0$ and 4–$r^2<0$, hence $r\in$(–$\infty$,–2).
Substitute Eq.(62) into second inequality of system Ineq.(60):

$$2-r^2-5\cdot\frac{r+\sqrt{r^2-4}}{2r}+2r(r+\sqrt{r^2-4})-\frac{3}{2}(r^2+r\sqrt{r^2-4}-2)>0, \tag{67}$$

$$5-r^2-\frac{5\sqrt{r^2-4}}{r}+r\sqrt{r^2-4}>0, \tag{68}$$

$$\frac{(5-r^2)\cdot(r-\sqrt{r^2-4})}{r}>0. \tag{69}$$

If $r$>2 then $r$–$\sqrt{r^2-4}>0$. From Ineq.(69) follows that 5–$r^2>0$. This takes place if $r\in$(2,$\sqrt{5}$).
If $r$<–2 then $r$–$\sqrt{r^2-4}<0$. From Ineq.(69) follows that 5–$r^2>0$. This takes place if $r\in$(–$\sqrt{5}$,–2).
So we got that the points

$$x_{5,6}=\pm\sqrt{\frac{r+\sqrt{r^2-4}}{2r}} \tag{70}$$

are periodic attractors if $r\in$(–$\sqrt{5}$,–2)$\cup$(2,$\sqrt{5}$).
Let's go back to the system of inequalities of Ineq.(60). For

$$x_{7,8}=\pm\sqrt{\frac{r-\sqrt{r^2-4}}{2r}} \tag{71}$$

we have

$$x^2=\frac{r-\sqrt{r^2-4}}{2r}. \tag{72}$$

Substitute Eq.(72) it into first inequality Ineq.(60):

$$1-r^2-2\cdot\frac{r-\sqrt{r^2-4}}{r}+2r(r-\sqrt{r^2-4})-\frac{3}{2}(r^2-r\sqrt{r^2-4}-2)<0, \tag{73}$$

$$2-\frac{1}{2}r^2+2\frac{\sqrt{r^2-4}}{r}-\frac{1}{2}r\sqrt{r^2-4}<0, \tag{74}$$

$$\frac{r(4-r^2)+(4-r^2)\sqrt{r^2-4}}{r}<0, \tag{75}$$

$$\frac{(4-r^2)(r+\sqrt{r^2-4})}{r}<0. \tag{76}$$

If $r$>2 then $r$+$\sqrt{r^2-4}>0$ and 4–$r^2<0$, hence $r\in$(2,+$\infty$).
If $r$<–2 then $r$+$\sqrt{r^2-4}<0$ and 4–$r^2<0$, hence $r\in$(–$\infty$,–2).
Substitute Eq.(72) it into second inequality of Ineq.(60):

$$2-r^2-5\frac{r-\sqrt{r^2-4}}{2r}+2r(r-\sqrt{r^2-4})-\frac{3}{2}(r^2-r\sqrt{r^2-4}-2)>0, \tag{77}$$

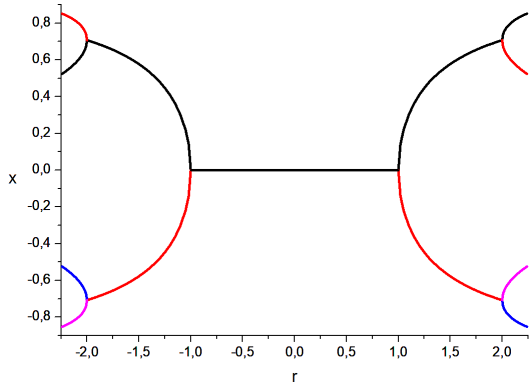


Fig. 4. Bifurcation diagram for recurrent sequence $x_{t+1} = r\cdot x_t \cdot(1 - x_t^2)$ at the interval $(-\sqrt{5},\sqrt{5})$.

$$5 - r^2 + \frac{5\sqrt{r^2-4}}{r} - r\sqrt{r^2-4} > 0, \tag{78}$$

$$\frac{(5-r^2)\cdot(r+\sqrt{r^2-4})}{r} > 0. \tag{79}$$

If $r$>2 then $r$+$\sqrt{r^2-4} > 0$. From Ineq.(69) follows that 5–$r^2 > 0$. This takes place if $r\in(2,\sqrt{5})$. If $r$<–2 then $r$+$\sqrt{r^2-4} < 0$. From Ineq.(69) follows that 5–$r^2 > 0$. This takes place if $r\in(-\sqrt{5},-2)$. So we got that the points

$$x_{7,8} = \pm\sqrt{\frac{r-\sqrt{r^2-4}}{2r}} \tag{80}$$

are periodic attractors if $r\in(-\sqrt{5},-2)\cup(2,\sqrt{5})$.
Thus, we have established that points

$$x_{5,6,7,8} = \pm\sqrt{\frac{r\pm\sqrt{r^2-4}}{2r}} \tag{81}$$

are periodic attractors if $r\in(-\sqrt{5},-2)\cup(2,\sqrt{5})$.
For recurrent sequence $x_{t+1} = r\cdot x_t\cdot(1-x_t^2)$ the bifurcation diagram at the interval $(-\sqrt{5},\sqrt{5})$ was depicted as presented in Fig. 4. Bifurcation diagram with period doubling 1, 2, 4 was obtained in analytical form solving 8-th degree polynomial equation. Strong expressed period doubling is presented at points $r$=1 and $r$=2.
Figs. 5, 6, 7, 8 represent graphical solutions of two functions $y = x$ and $y = \Phi^2$(x) at different $r$: $r$=2.0, $r$=2.2, $r$=2.23, and $r$=2.3 respectively. For $r$=2.0 (Fig. 5), five crossing points are present, but zero periodic attractors. For $r$=2.2 (Fig. 6), nine crossing points are present, but four of them are periodic attractors. For $r$=2.23 (Fig. 7), nine crossing points are present, but four of them are periodic attractors. For $r$=2.3 (Fig. 8), nine crossing points are present, but none of them are periodic attractors.

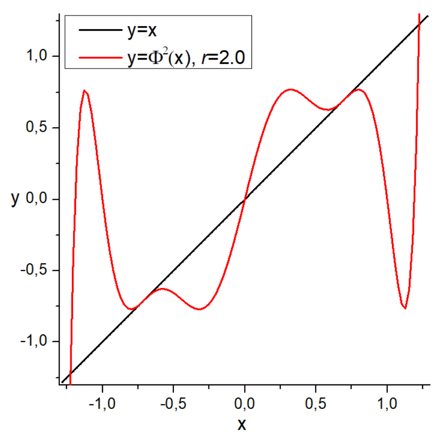


Fig. 5. $y = x$ and $y = \Phi^2$(x) at $r$=2. Five crossing points, but zero periodic attractors.

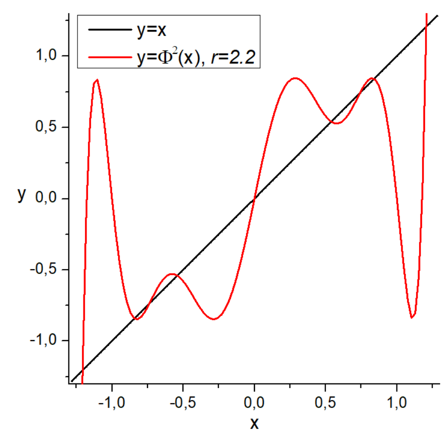


Fig. 6. $y = x$ and $y = \Phi^2$(x) at $r$=2.2. Nine crossing points, four of them are periodic attractors.

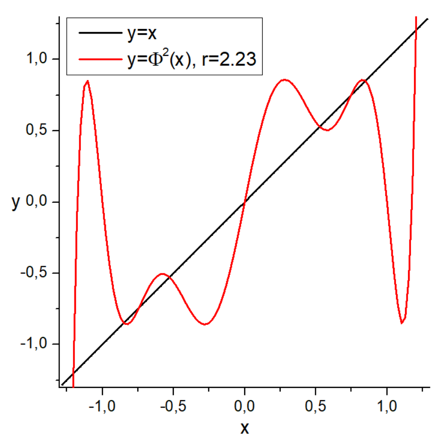


Fig. 7. $y = x$ and $y = \Phi^2$(x) at $r$=2.23. Nine crossing points, four of them are periodic attractors.

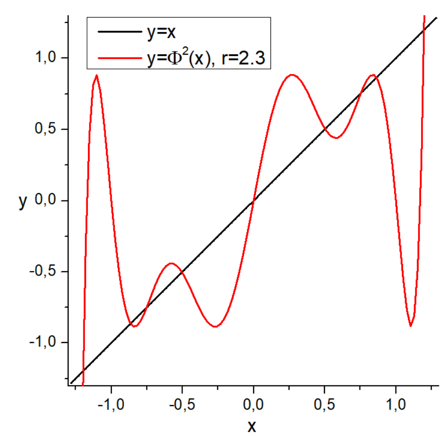


Fig. 8. $y = x$ and $y = \Phi^2$(x) at $r$=2.3. Nine crossing points, but none of them are periodic attractors.

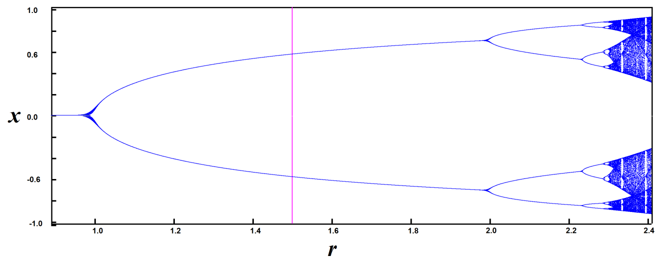


Fig. 9. Finite State Diagram of sequence $x_{t+1} = r \cdot x_t \cdot (1 - x_t^2)$, $t$=0, 1, 2, . . . . Values in interval (0;1) (top branch) were generated using $x_0$=0.3, and values in interval (-1;0) (bottom branch) were generated using $x_0$=–0.3.

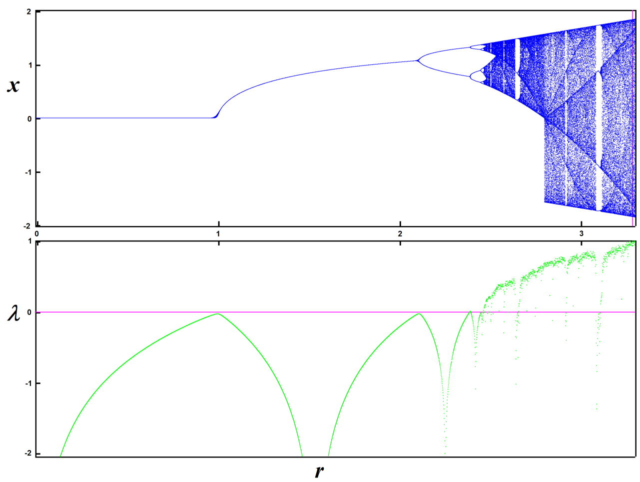


Fig. 10. Finite State Diagram (top) and distribution of Lyapunov exponent index (bottom) of recurrent sequence $x_{t+1} = r{\cdot}x_t \cdot\cos x_t$, $t$=0, 1, 2, . . . , $x_0$ = 0.5.

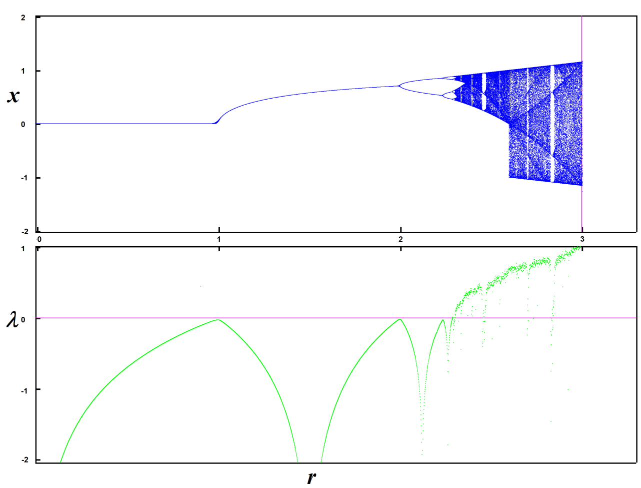


Fig. 11. Finite State Diagram (top) and distribution of Lyapunov exponent index (bottom) of recurrent sequence $x_{t+1} = r{\cdot}x_t{\cdot}(1 - x_t^2)$, $t$=0, 1, 2, . . . , $x_0$ = 0.5.

## 5. Approximation methods for visualization

Initial estimation of recurrent sequence properties could be done using previously presented tool *QUATTRO* [27] where several behaviours such as Finite State Diagram and of Lyapunov exponent index are presented as the fingerprints of recurrent relations. Fig. 9 represent the Finite State Diagram generated using recurrent sequence $x_{t+1} = r \cdot x_t \cdot (1 - x_t^2)$. Values in interval (0;1) (top branch) were generated using initial value $x_0$=0.3, and corresponding values in interval (–1;0) (bottom branch) were generated using $x_0$=–0.3.

Figs. 10 and 11 represent the Finite State Diagram and distribution of Lyapunov exponent index $\lambda(x_0)$ of two recurrent relations $x_{t+1} = r \cdot x_t \cdot \cos x_t$, and $x_{t+1} = r \cdot x_t \cdot (1 - x_t^2)$, $t$=0, 1, 2, . . ., respectively. In both cases, initial value $x_0$ = 0.5. Both Finite State Diagrams look quite similar. Their different ranges of values are explained by the normalization of the scales, see Eq.(20).

Fig. 11 (bottom) represents the distribution of Lyapunov Exponent index:

$$\lambda(x_0) = \lim_{t\to\infty} \left( \frac{1}{t} \sum_{i=0}^{t-1} \ln \left| \Phi'(x_i) \right| \right). \tag{82}$$

At $r$=1.5, value of distribution $\lambda(x_0)$ tends to $-\infty$ which indicates the absence of chaotic dependence on initial $x_0$. Distribution of Lyapunov Exponent index $\lambda(x_0)$ characterizes the behaviour of chaotic dynamics as well as various forms of stabilization or synchronization. Positive value of Lyapunov exponent index indicates chaotic behaviour of the sequence according to sensitive dependence on initial $x_0$.

Figs. 12, 13 represent CoWeb plots of the recurrent sequence $x_{t+1} = r \cdot x_t \cdot (1 - x_t^2)$, $t$=0, 1, 2, . . ., $x_0$ = 0.5, when $r_1$=1.9, $r_2$=2.2, $r_3$=2.26, $r_4$=3.0. Different character of sequence convergence could be established. 50 iterations is enougth to describe the trending manner. Fig. 12a represents visualization of the fixed point attractor ($r_1$=1.9). Figs. 12b and 13a represent visualization of two types of periodic attractors (period doubling 2 for $r_2$=2.2 and period doubling 4 for $r_3$=2.26). For $r_3$=3.0, chaotic dependence occurs - see Fig. 13b.

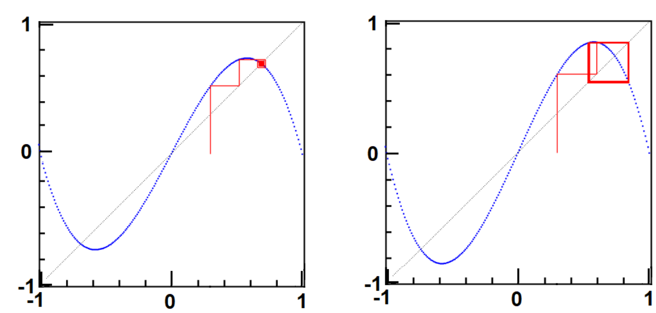

a) $r_1$=1.9; b) $r_2$=2.2.

Fig. 12. CoWeb plot of recurrent sequence $x_{t+1} = r{\cdot}\, x_t \cdot (1 - x_t^2)$, $t$=0, 1, 2, . . ., $x_0$ = 0.3. 50 iterations were used.

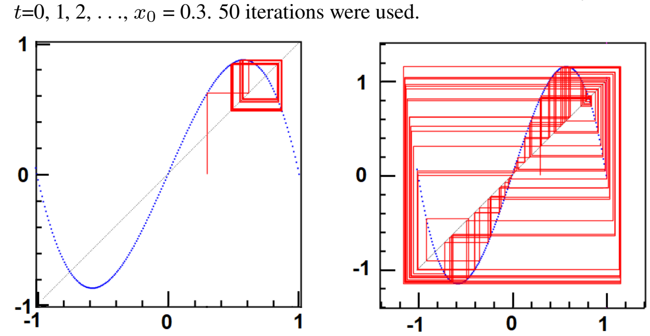

a) $r_3$=2.26; b) $r_4$=3.0.

Fig. 13. CoWeb plot of recurrent sequence $x_{t+1} = r{\cdot}\, x_t \cdot (1 - x_t^2)$, $t$=0, 1, 2, . . ., $x_0$ = 0.3. 50 iterations were used.

## Conclusions

By analysing of recurrent sequence generated by trigonometric function $F(x) = r \cdot x \cdot \cos x$ some problems arise related to second composite $F^2(x)$ due to the complexity of expressions. Using MacLaurin approximation for function $\cos x$, the dynamic behavior of the recurrent sequence was studied in the same manner as discrete analogue of Verhulst equation [10]. We presented the bifurcation diagram for recurrent sequence generated by power function $\Phi(x) = r\cdot x\cdot (1 - x^2)$. Function $\Phi(x)$ and its second composite $\Phi^2(x)$ were used. Analytical solutions of equation $x = \Phi^2(x)$ allows us to establish the fixed point attractors and periodic attractors in the interval $(-\sqrt{5}, \sqrt{5})$. Bifurcation diagram with period doubling 1, 2, 4 was obtained in analytical form solving 8-th degree polynomial equation and compared with Finite State diagram as an aproximate analogue.

## Authors' contributions

Jelena Kozmina formulated general idea, derived mathematical formulas and validated results. Alytis Gruodis presented literature review, realized the graphical implementation and prepared analysis of data. Both authors reviewed and approved the final manuscript.

## Conflicts of interest

Authors declared at they have no conflicts of interest.

## References


1. Bruno Gonpe Tafo, J.; Nana, L.; Tabi, C. B.; Kofané, T. C. (2020) Nonlinear Dynamical Regimes and Control of Turbulence through the Complex Ginzburg-Landau Equation - *Research Advances in Chaos Theory* IntechOpen - doi:10.5772/intechopen.88053.
2. Tzamal- Odysseas, M. (2014) Energy transfer and dissipation in nonlinear oscillators. PhD theses - Aristotle University of Thessaloniki, Greece, 2014.
3. Elaydi, S. (2005) An introduction to difference equations 3rd ed. - Springer Science: Business Media, Inc., 2005.
4. Devaney , R. L. (2020) A First Course in Chaotic Dynamical Systems. Theory and Experiment. 2nd Edition - Taylor & Francis Group, LLC, 2020.
5. Chen, Y.; Qian, Y.; Cui, X. (2022) Time series reconstructing using calibrated reservoir computing - *Scientific Reports* 12 (2022) 16318 - https://doi.org/10.1038/s41598-022-20331-3
6. Tronci, S.; Giona, M.; Baratti, R. (2003) Reconstruction of chaotic time series by neural models: a case study - *Neurocomputing* 55 (2003)581-591 - https://doi.org/10.1016/S0925-2312(03)00394-1.
7. Boutsinas, B.; Vrahatis, M.N. (2001) Artificial nonmonotonic neural networks - *Artificial Intelligence* 132(2001)1-38 - https://doi.org/10.1016/S0004-3702(01)00126-6.
8. Bakas, I.; Kontoleon, K.J. (2021) Performance Evaluation of Artificial Neural Networks (ANN) Predicting Heat Transfer through Masonry Walls Exposed to Fire - *Applied Science* 11 (2021)11435 - https://doi.org/10.3390/app112311435.
9. Gómez-Ramos, E.; Venegas-Martínez, F. (2013) A Review of Artificial Neural Networks: How Well Do They Perform in Forecasting Time Series? - *Analitika, Revista de analisis estadistico* 3 (2013)7-15
10. Kozmina, Y. (2018) Discrete Analogue of the Verhulst Equation and Attractors. Methodological Aspects of Teaching - *Innovative Infotechnologies for Science, Business and Education* 1(24) (2018) 3-12.
11. Kozmina, Y.; Gruodis, A. (2020) QUATTRO-20: advanced tool for estimation of the recurrent sequences - In: 18th International Conference "Information Tehnologies and Management", April 23-24, 2020, ISMA University of Applied Science, Riga, Latvia.
12. Kozmina, J.; Gruodis, A. (2023) Tool QUATTRO-20 for Examining of the Recurrent Sequencies Generated by Discrete Analogue of the Verhulst Equation. - *Applied Business: Issues & Solutions* 1(2023)16–29 - https://doi.org/10.57005/ab.2023.1.3.
13. Dosly, O.; Pechancova, S. (2006) Trigonometric Recurrence Relations and Tridiagonal Trigonometric Matrices - *International Journal of Difference Equations* 1 (2006) 19–29.
14. Brooke, K.; Saucedo, D.; Xu, C. (2017) Second-Order Linear Recurrence Relations and Periodicity - *The Onyx Review: The Interdisciplinary Research Journal* 2(2017) 7-12.
15. Farris, M.; Luntzlara, N.; Miller, S.; Lily, S.; Mengxi, W. (2021) Recurrence relations and Benford's law - *Statistical Methods & Applications* 797 (2021) 1613-981X - https://doi.org/10.1007/s10260-020-00547-1
16. Būdienė, G.; Gruodis, A. (2016) Zipf and related scaling laws. 3. Literature overview of multidisciplinary applications (from informational aspects to energetic aspects) - *Innovative Infotechnologies for Science, Business and Education* ISSN 2029-1035 – 2(21)(2016)12-19.
17. Andrianov, I.; Starushenko, G.; Kvitka, S.; Khajiyeva, K. (2019) The Verhulst-Like Equations: Integrable O$\Delta$E and ODE with Chaotic Behavior - *Symmetry* 11 (2019) 1446 - doi:10.3390/sym11121446.
18. Gutierrez, M. R.; Reyes, M.A.; Rosu, H.C. (2010) A note on Verhulst's logistic equation and related logistic maps- *J. Phys. A* 43 (2010) 205204.
19. Ragulskis, M.; Navickas, Z. (2011) The rank of a sequence as an indicator of chaos in discrete nonlinear dynamical systems - *Communications in Nonlinear Science and Numerical Simulation* 16(2011) 2894-2906 - https://doi.org/10.1016/j.cnsns.2010.10.008.
20. Hikihara, T.; Holmes, P.; Kambe, T.; Rega, G. (2012) Introduction to the focus issue: Fifty years of chaos: Applied and theoretical - *Chaos* 22(2012) 047501 - https://doi.org/10.1063/1.4769035
21. Ditto, W.; Munakata, T. (1995) Principles and Applications of Chaotic Systems - *Communications of the ACM* 38(1995) 96-102.
22. Nosrati, K.; Volos, C. (2018) Bifurcation Analysis and Chaotic Behaviors of Fractional-Order Singular Biological Systems - In: Nonlinear Dynamical Systems with Self-Excited and Hidden Attractors. Eds. Viet-Thanh Pham, Sundarapandian Vaidyanathan, Christos Volos, Tomasz Kapitaniak - Series: Studies in Systems, Decision and Control, Volume 133 - Springer International Publishing AG 2018.
23. Toker, D.; Sommer; F. T.; D'Esposito, M. (2020) A simple method for detecting chaos in nature - *Communications Biology* (2020) 3:11 - https://doi.org/10.1038/s42003-019-0715.
24. Fehrle, D.; Heiberger, C.; Huber, J. (2020) Polynomial chaos expansion: Efficient evaluation and estimation of computational models - *BGPE* Discussion Paper, No. 202, Friedrich-Alexander-Universität Erlangen-Nürnberg, Erlangen und Nürnberg - http://hdl.handle.net/10419/237993
25. Kozmina, Y.; Gruodis, A. (2019) Number generation based on the chaotic sequences - In: The 17th International Scientific Conference "Information Technologies and Management - 2019", April 25-26, 2019, ISMA, Riga, Latvia - *Nano Technologies and Computer Modelling* (2019)17-18.
26. Alawida, M.; Samsudin, A.; Teh, J. S. (2019) Enhancing Unimodal Digital Chaotic Maps through Hybridization - *Nonlinear Dynamics* 96 (2019) 601–613 - https://doi.org/10.1007/s11071-019-04809-w
27. Kozmina, J.; Gruodis A. (2020) *QUATTRO-20* - WinApi program. - https://github.com/Alytis/QUATTRO-20.